data

MDPI

Data Descriptor

Global Dataset of Extreme Sea Levels and Coastal Flood Impacts over the 21st Century

Ebru Kirezci [1], Ian Young [1,*], Roshanka Ranasinghe [1,2,3], Yiqun Chen [1], Yibo Zhang [1] and Abbas Rajabifard [1]

[1] Department of Infrastructure Engineering, University of Melbourne, Melbourne, VIC 3010, Australia; ebrukirezci@gmail.com (E.K.); r.ranasinghe@un-ihe.org (R.R.); yiqun.c@unimelb.edu.au (Y.C.); yibo.zhang1@unimelb.edu.au (Y.Z.); abbas.r@unimelb.edu.au (A.R.)
[2] Department of Coastal and Urban Risk & Resilience, IHE Delft Institute for Water Education, P.O. Box 3015, 2601 DA Delft, The Netherlands
[3] Resilient Ports and Coasts, Deltares, P.O. Box 177, 2600 MH Delft, The Netherlands
* Correspondence: ian.young@unimelb.edu.au

Abstract: A global database of coastal flooding impacts resulting from extreme sea levels is developed for the present day and for the years 2050 and 2100. The database consists of three sub-datasets: the extreme sea levels, the coastal areas flooded by these extreme sea levels, and the resulting socioeconomic implications. The extreme sea levels consider the processes of storm surge, tide levels, breaking wave setup and relative sea level rise. The socioeconomic implications are expressed in terms of Expected Annual Population Affected (EAPA) and Expected Annual Damage (EAD), and presented at the global, regional and national scales. The EAPA and EAD are determined both for existing coastal defence levels and assuming two plausible adaptation scenarios, along with socioeconomic development narratives. All the sub-datasets can be visualized with a Digital Twin platform based on a GIS-based mapping host. This publicly available database provides a first-pass assessment, enabling users to extract and identify global and national coastal hotspots under different projections of sea level rise and socioeconomic developments.

Dataset: https://doi.org/10.26188/25874179.v1

Keywords: extreme sea levels; coastal flooding; sea level rise

Academic Editor: Jamal Jokar Arsanjani

Received: 29 October 2024
Revised: 18 January 2025
Accepted: 20 January 2025
Published: 28 January 2025

Citation: Kirezci, E.; Young, I.; Ranasinghe, R.; Chen, Y.; Zhang, Y.; Rajabifard, A. Global Dataset of Extreme Sea Levels and Coastal Flood Impacts over the 21st Century. *Data* **2025**, *10*, 15. https://doi.org/10.3390/data10020015

1. Summary

Sea level rise is a consequential impact of global climate change. Over the period 2006–2015, the global mean sea level (MSL) has increased at an average rate of 0.36 cm/year, with acceleration observed [1]. It is anticipated that even if the Paris Agreement limit of 1.5 °C above pre-industrial levels is achieved, the rate of global MSL rise will increase over the 21st century [2,3]. Projected climate change will enhance both the frequency and severity of extreme sea levels (ESLs) [1,3–6] globally, which mainly result from storm surges and/or extreme wave conditions coinciding with high tides. Over the 21st century, ESL combined with relative sea level rise (RSLR), may result in increased flood areas with potentially unprecedented societal and economic impacts. Effective and ambitious adaptation and mitigation strategies are likely to be required to address such impacts [6]. Low-elevation coastal zones (LECZs), which are defined as, ocean connected coastal areas below 10 m above MSL, will be most impacted by such flooding, annually putting at risk more than

34 million people and $US 307B worth of global wealth [7]. Future socioeconomic developments are likely to increase populations and infrastructure assets in LECZs, exacerbating the potential impacts of coastal flooding.

To inform and guide policy directions for LECZs, it is essential that estimates of the long-term extent of episodic coastal extremes and resulting socioeconomic impacts in LECZs are available. Such analysis needs to be both at the local scale—to guide local development, but also at the national and global scales—to inform geopolitical developments, including regional to international policy-making processes. In the last decade, there has been an increased effort to estimate extreme sea levels at regional [8–10] and global [4,5,11,12] scales, in terms of present and future conditions, under the projected influence of climate change. Global coastal impact analyses [5,13–15] are essential first-pass assessments to identify "hotspots" that are at greatest risk and more vulnerable to projected sea level rise and ESLs. Such assessments improve the ability to predict present and future ESL magnitudes and their implications at these locations and enable mitigation of potential adverse impacts. To this end, it is crucial to identify the global present and projected ESL, their corresponding coastal flood extents and resulting socioeconomic impacts.

Kirezci et al. [5,7] presented global estimations of ESLs, the coastal flood extent for a variety of return period levels, and estimates of Expected Annual People Affected (EAPA) and Expected Annual Damage (EAD) for the present day (i.e., 2015), and future times (i.e., 2050 and 2100). Kirezci et al. [5] also identified global "hotspots" of coastal flooding for 100-year return period (RP) ESLs; however, they assumed no existing flood protection. Kirezci et al. [7] extended this analysis by including estimated flood protection, both for the present and future adaptation considerations.

To account for regional relative sea level rise (RSLR), projections from both Intergovernmental Panel on Climate Change (IPCC)—Special Report on the Ocean and Cryosphere in a Changing Climate (SROCC) [1] and IPCC AR5 (Assessment Report 5) [16] (see "Datasets" and "Methods" Section) under Representative Concentration Pathways (RCPs) of 2.6 (low-end), 4.5 (mid-level), and 8.5 (high-end) were used. Plausible future adaptation strategies were defined using three possible adaptation scenarios; (i) no socioeconomic change, (ii) adaptation matching ESL change, and (iii) no additional adaptation (as defined in Kirezci et al. [7]; also see Section 3). The historical and future global inundation extents were determined from the ESLs attributed to 9864 Dynamic Interactive Vulnerability Assessment Database (DIVA) coastal segments and computed using a bathtub approach for the different adaptation scenarios. To account for future socioeconomic development (cases ii and iii), Shared Socioeconomic Pathways (SSPs) were combined with Representative Concentration Pathways (RCPs) (see Section 3). Finally, the estimated values of EAPA and EAD were given at regional and national scales for each adaptation scenario and aggregated to global values. As a result, three sub-datasets were produced, i.e., (i) ESLs, (ii) corresponding inundation extent, and (iii) EAPA/EAD values per nation.

This Data Descriptor describes and makes available the datasets developed, validated and described in detail by Kirezci et al. [5,7]. The subsequent sections provide an overview of the data sources used, the methods applied to these sources to obtain the final datasets and the limitations necessary for the construction of such a global dataset. In addition, a data visualization platform is described. More extensive descriptions of the approaches used, validation, and limitations can be found in Kirezci et al. [5,7]. The reader is encouraged to consult these source references in conjunction with this Data Descriptor. The dataset is intended to provide a global-scale resource to assess the potential impacts of projected sea level rise on coastal communities. These results are provided at more than 9000 coastal locations. In addition to defining projected changes in ESLs, the data estimate the extent

of resulting coastal flooding the number of people impacted annually and the expected annual economic damage to coastal infrastructure.

2. Data Description

2.1. Description of the Datasets Used

Figure 1 shows the database in a diagrammatic form, indicating each of the public domain datasets used to compile the final datasets and the sequential steps required to produce the final products. The database is divided into three sub-datasets representing extreme sea levels, coastal flooding extent, and socioeconomic impacts. The coloured boxes in Figure 1 show the data products contained within the database. The extreme sea levels represent the 1 in 100-year sea level for both the present day and for future periods under a number of different climate change projections. The coastal flooding extent considers coastal topography to estimate the regions flooded by the projected extreme sea levels. This analysis includes estimates of coastal defences in place around the world. Finally, the numbers of people potentially impacted and the Expected Annual Damage are estimated.

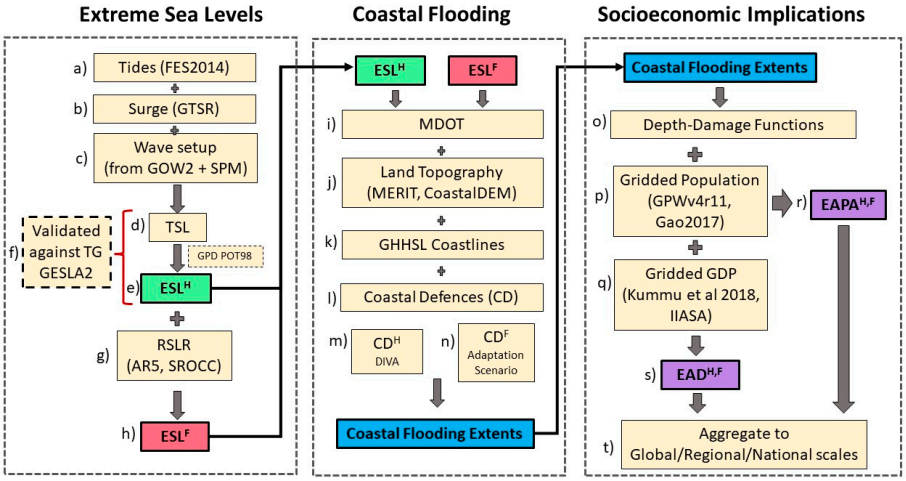

Figure 1. Flowchart representation of the processes used in the production of the ESL, flooding extent and EAPA/EAD datasets. Coloured boxes show the datasets available within this database. The abbreviations and superscripts are explained throughout the paper.

2.1.1. Extreme Sea Level (ESL) Analysis

The extreme sea level analysis is based on a time series of tide, storm surge, and wave setup (see Section 3; Equation (1)) together with relative sea level rise (see Section 3; Equation (2)) [5,7].

Tide: The global tidal elevations were obtained from FES2014 [17], accessible at https://www.aviso.altimetry.fr/en/data/products/auxiliary-products/global-tide-fes/description-fes2014.html (accessed on 25 October 2024). FES2014 represents a finite element hydrodynamic model designed to solve tidal barotropic equations while assimilating in situ tide gauge and altimeter data. This dataset has a spatial resolution of 1/16°.

Storm surge: The global storm surge levels were acquired from the Global Tide and Surge Reanalysis (GTSR) dataset [11]. This dataset was produced using Delft3D FM [11], featuring a spatial resolution ranging from 50 km in deep ocean regions to 5 km in coastal areas. The model was forced with meteorological information from ERA-Interim [18]. The surge time-series data from GTSR were downscaled at 10 min resolution over the 36-year period 1979–2014.

Wave setup: The determination of wave contributions to the time-averaged sea level used model data of significant wave height obtained from the GOW2 [19] dataset. Wave setup was estimated using the SPM method [20] with a globally representative bed slope

of 1/30. An in-depth examination, conducted by Kirezci et al. [5] explored the impact of alternative bed slopes (1/15 and 1/100). To address uncertainty related to the adopted wave setup methodologies, an alternative method proposed by Stockdon et al. [21] was also considered. The study concluded that, on a global scale, there are only small differences between the two methods for ESL^{H100} [5], where the superscript indicates a 1 in 100-year return level for the historical period (see Section 3).

Regional relative sea level rise: To incorporate estimates of future regional relative sea level rise, two global datasets, namely SROCC [1] and AR5 [16], were employed for RCPs 2.6, 4.5, and 8.5 by Kirezci et al. [5,7]. The use of AR5 was so as to facilitate comparisons with previous studies. The AR5 computations are not provided in the present database. A notable difference between the sea level rise (RSLR) projections from AR5 and SROCC is the inclusion of more recent projections of the Antarctic Ice Sheet (AIS) contribution to RSLR in the SROCC dataset [1]. By the year 2100, IPCC AR5 projects a global mean sea level rise of 0.28 m/0.52 m to 0.61 m/0.98 m for RCP 2.6 and RCP 8.5, respectively, while SROCC projects a range of 0.29 m/0.59 m to 0.61 m/1.10 m for the same RCPs.

Tide gauge data: A quasi-global dataset of tide gauge observations, GESLA2 [22], was utilized to assess ESL^{H100} through the analysis of recorded time series. This functioned as a method to validate the extreme value estimates derived from the combined model time series (T+S+WS, see Section 3 Equation (1)). This validation can be found in Kirezci et al. [5].

2.1.2. Coastal Inundation Extent

Noting the estimated extreme sea levels described above, the coastal inundation flooding extent was calculated using the following datasets.

MSL data: The reference datum for the historical time series of total sea level (TSL) and, consequently, extreme sea level (ESL), are the mean sea level (MSL). To align the land topography with ESL, the Mean Dynamic Ocean Topography (MDOT) [23] is applied. MDOT represents the difference between the time-averaged sea surface and the geoid.

Land topography: Coastal land elevations were derived from the Digital Elevation Model (DEM) entitled Multi-Error Removed Improved Terrain (MERIT) [24]. This DEM covers land areas from 90°N to 60°S and was developed by refining existing spaceborne DEMs (SRTM3 v2.1 and AW3D-30m v1 [25,26]) and eliminating significant error components. The MERIT DEM uses a 3-arcsecond (~90 m) horizontal resolution and adheres to the vertical datum of EGM96. Note that an alternative DEM, CoastalDEM v2.1 [27], was also utilized by Kirezci et al. [5,7] for comparison purposes. The output from this DEM is not included in the present database.

Coastline data: The Global Self-consistent Hierarchical High-resolution Geography (GSHHG) [28] dataset was used to define the global coastline for calculations of coastal flooding extent, and to bring a variety of global data layers to a consistent coastline position.

Coastal Defences: Estimates of present day global coastal defences were obtained from the DIVA [15,29], where defence levels are defined in terms of return periods of extreme sea levels (e.g., protection level for a 50-year return period) at each DIVA location. These return periods were converted to protection levels (expressed in metres) by utilizing the associated Generalized Pareto Distribution (GPD) probability distribution function at each coastal location, as detailed in the Section 3.

2.1.3. Socioeconomic Impacts

Such coastal inundation will result in socioeconomic impacts on coastal communities. These impacts are quantified in terms of the EAPA and EAD [15,30] evaluated using the following datasets.

Population: Two global gridded population datasets were employed to characterize current and projected future conditions. For the present day (2015), the population count database was taken from the NASA Socioeconomic Data and Applications Center (SEDAC) GPWv4 Rev. 11, utilizing census data from 2015 on a 30-arcsecond grid (~1 km at the equator). To account for projected population variations in 2050 and 2100, the gridded population data developed by Gao [31] for SSP narratives SSP1, SSP3, and SSP5 were utilized.

Gross Domestic Product: The GDP data for the present day (2015) were extracted from Kummu et al. [32]. This dataset includes GDP per capita (PPP) information on a 5-arcminute grid, downscaled to 30 arcseconds for consistency with other datasets. Projections for future changes in global GDP were obtained from IIASA [33] (https://tntcat.iiasa.ac.at/SspDb/, accessed on 25 October 2024).

2.2. Data Records

An overview of the structure of the data records is presented in Tables 1–3. As noted previously, the data are arranged in three sub-datasets: (a) extreme sea levels (Table 1), (b) coastal flooding extent (Table 2), and (c) socioeconomic impacts (Table 3). The ESL data are arranged as a single NetCDF file (.nc) consisting of ESL for return values of n = 1,10,100,1000 and 10,000 years for the present day (2015) and 2050 and 2100. For both future periods, ESL values are provided for three Representative Concentration Pathways (RCPs): RCP2.6, RCP4.5, and RCP8.5. This NetCDF file contains the data for all 9864 DIVA points, and the latitude, and longitude information for each point. ESLs are referenced to MSL.

Table 1. Summary Data record structure for the Global ESLs.

	Year	RCP/SSP Narratives	Return Periods
ESLdata.nc (Extreme Sea Levels)	Baseline	-	1, 10, 100, 1000, 10,000
	2050 2100	RCP 2.6 RCP 4.5 RCP 8.5	1, 10, 100, 1000, 10,000

Table 2. Summary Data record structure for the Global coastal flood extent.

	Year	Adaptation Scenario Folder Path	RCP/SSP Narratives	Return Periods
CoastalFloodAreas (shapefile directory for the coastal flooded areas)	Baseline	**Baseline** (Coastal flood areas for the Baseline [Present] case)	-	1, 10, 100, 1000, 10,000
	2050 2100	**Without_Adaptation** (Coastal flood areas under "No Socioeconomic Change" and "No Additional Adaptation" cases)	RCP 2.6 RCP 4.5 RCP 8.5	1, 10, 100, 1000, 10,000
		With_Adaptation (Coastal Flood areas under "Adaptation Matching ESL Change" case)		

Table 3. Summary Data record structure for the Global EAPA/EAD.

	Data List	Year	Adaptation Scenario	RCP/SSP Narratives
EAPAandEAD_Tables (Excel Spreadsheet file directory for EAPA and EAD values at IPCC AR6 Regions and at National Scales)	- National IPCC AR6 Regions	Baseline	-	-
		2050 2100	No Socioeconomic Change	RCP2.6 RCP4.5 RCP8.5
			Adaptation Matching ESL Change	SSP1-2.6 SSP1-4.5 SSP3-8.5 SSP5-8.5
			No Additional Adaptation	

The inundated areas associated with each ESL are presented as shapefiles (.shp) for the GIS software. Inundated areas are provided for: present day and future dates 2050 and 2100. For each of 2050 and 2100 flooding extent is defined for each RCP case (RCP2.6, RCP4.5, and RCP8.5). As the flooding extent depends on the level of flood protection, results for three adaptation scenarios are provided: no socioeconomic change, adaptation matching ESL change, and no additional adaptation [7]. Again, data are provided for return period values of n = 1, 10, 100, 1000, and 10,000 years.

The EAPA and EAD are provided in the form of Excel (.xlsx) spreadsheet tables for each AR6 region and each nation. Note that global values are provided in Kirezci et al. [7]. As EAPA and EAD are obtained by integration over all return periods, no data by return period are provided. However, the variables depend on the SSP pathway, which impacts population and GDP. Therefore, data are provided for the present day, 2050 and 2100, for each of the three adaptation scenarios considered and all RCP/SSP cases. Note that, the EAPA and EAD values for all the adaptation scenarios (for 2050 and 2100) are provided as relative to the present case (baseline).

The data for ESLs, flooded areas, and EAPA/EAD for each nation can be visualized using the Digital Twin platform which can be accessed through the publicly open URL link https://idigitaltwin.org/?view=coastalFloodViewer (accessed on 24 January 2025). The Digital Twin platform renders the geospatial data as layers, allowing the layers to be stacked. This enables users to identify and compare the differences between RCPs, adaptation scenarios, years and return periods (see Section 4). The datasets can be downloaded from (https://doi.org/10.26188/25874179.v1).

3. Methods

Kirezci et al. [5,7] describe in detail how the various datasets are combined and also validate each of the intermediate steps in detail against a range of independent sources. Below, these steps are briefly summarized to aid in the use and understanding of the data provided. The reader is referred to Kirezci et al. [5,7] for a more detailed discussion.

3.1. Present and Future Projections of ESL

In most cases, ESLs occur when high tides coincide with climate extremes such as storm surges and extreme waves. Therefore, each of the components of a total sea level (TSL) needs to be evaluated simultaneously. Kirezci et al. [5] combined global datasets of tide (T), storm surge (S) and wave setup (WS) to find the historical TSL at a total of 9864 locations defined by the Dynamic Interactive Vulnerability Assessment dataset (these coastal locations are referred to as "DIVA points") [29,34]. The sea level components were

combined as a linear summation, as in Equation (1). The details of the datasets for the individual components are described in the "Datasets" Section.

$$TSL = T + S + WS \quad (1)$$

The probability of occurrence of ESLs can be represented in terms of the return period, such as a 1-in-a-100-year event (i.e., RP100). Kirezci et al. [5,7] computed ESLs at various probability levels by fitting a Generalized Pareto Distribution (GPD) to the TSL at each DIVA location. Kirezci et al. [5] investigated various extreme value distributions and concluded that the GPD fitted to peak over threshold data gave the best agreement with tide gauge data from 681 sites [22]. The ESLs estimated in this manner have been termed ESL^H, with the superscript "H" indicating they refer to the historical period, here taken as 2015. To determine the future estimations of ESLs, (i.e., ESL^F), the regional relative sea level rise projections (RSLRs) were added to ESL^H (Equation (2)). RSLR was here estimated globally from SROCC [1] and AR5 [16] in 2050 and 2100. Utilizing two datasets for RSLR enables an analysis of the uncertainties associated with the RSLR projections, which Kirezci et al. [7] discuss in detail.

$$ESL^F = ESL^H + RSLR \quad (2)$$

The approach given in Equation (2) assumes that there is no change in the magnitude of the components in Equation (1) from 2015 to the future dates when ESL^F is estimated (2050 or 2100). Kirezci et al. [5] showed that estimates of such changes are small compared to RSLR and potential uncertainties in the Extreme Value Analysis.

The TSLs and ESLs were validated against tide gauge observations, showing a generally good agreement. A detailed discussion of this validation can be found in the Supplementary Materials, Section S.1.1, Validation of Historical Sea Level Timeseries (TSL) and ESL Against Tide Gauge Recordings. Additionally, a comparative analysis with previous global studies on ESL^H was conducted, revealing consistent alignment between our ESL^H findings and those of earlier research (refer to Supplementary Materials Section S.1.3, Comparison with Previous Studies: ESL).

In the database presented here, ESLs are evaluated at DIVA points for return periods (RP) of 1, 10, 100, 1000, and 10,000 years, under present conditions (baseline) and projected for 2050 and 2100.

3.2. Episodic Coastal Flooding

Estimates of the episodic coastal flooding extent were obtained for values of ESL^H and ESL^F by assigning areal extent at each of the DIVA points using Thiessen polygons and a bathtub assumption. The details of the approach and the resulting limitations are discussed by Kirezci et al. [5]. For the present day, coastal defence levels were taken from Hinkel et al. [15], estimated using a stylized model of protection based on local floodplain population density and local GDP per capita [35], complemented with protection levels for the largest 136 coastal cities of Hallegatte et al. [36]. The coastal defence dataset was presented in the form of the return period of the protection levels (e.g., 50-year return period protection level), which Kirezci et al. [7] converted into coastal defence heights by utilizing the probability distribution function defined at each coastal location and previously used to estimate ESL^H. Kirezci et al. [7] assume an area is inundated when the ESL exceeds the coastal defence level and the land topography elevation is lower than that ESL. Once overtopped, the coastal flood depth is taken to be equal to ESL minus the land elevation.

To account for future adaptation scenarios, Kirezci et al. [7] assumed three plausible adaptation pathways: (i) the no-socioeconomic-change case, where population, GDP and adaptation levels remain constant at values for the baseline year (here taken as 2015) and

only the ESL varies for each of Representative Concentration Pathways considered: RCP2.6, 4.5 and 8.5; (ii) the case of adaptation matching ESL changes, where it is assumed that society responds to future sea level rise by introducing adaptation in the form of raising existing and building new defences, such that the height of enhanced coastal protection matches the increase in ESL; and (iii) the no-additional-adaptation case, where current defences are maintained but not upgraded and no new defences are constructed, whilst population and GDP change.

3.3. Expected Annual People Affected (EAPA) and Expected Annual Damage (EAD)

Kirezci et al. [5,7] evaluated the populations and infrastructure impacted by a given probability of exceedance event. In order to estimate the damage associated with this event, however, it is necessary to assume a depth-damage function, a commonly assumed form is given in Equation (3) [7,15].

$$V = d/d + 1 \quad (3)$$

Here, V is the proportion of the value of the assets damaged, due to flood depth, d, computed from ESL^{H}_{n} or ESL^{F}_{n} values, where n is the return period, related to the probability of exceedance, P, by P = 1/n. The appropriateness of this function is considered in detail by Kirezci et al. [7].

To assess Expected Annual Damage (EAD) and Expected Annual Population Affected (EAPA), the computational process involves calculating flooded areas, determining flood depths, and applying the depth–damage function (Equation (3)) for the return periods given in "Methods"—Section 1. The relationship between asset exposure and population, along with Gross Domestic Product per capita, is utilized to estimate the value of exposed assets [7,15,37–39] for each computational grid cell. This approach is implemented with discrete gridded data and involves summing over all probability of exceedance levels. This computational approach allows for global-scale application by aggregating values utilizing many gridded datasets. A detailed step-by-step methodology is given by Kirezci et al. [7].

The EAPA and EAD outputs in this analysis were compared with previous studies, specifically focusing on the "No Additional Adaptation" scenario, as it is the most widely assessed and commonly overlapping adaptation scenario. The EAPA values for this scenario in the present dataset show consistency with findings from earlier studies (see Supplementary Materials Section S.1.4, Comparison with Previous Studies: EAPA and EAD).

To illustrate how different coastal topography datasets (Digital Elevation Model—DEM) affect inundation extents and the resulting socioeconomic impacts, a similar analysis to presented here was conducted using the CoastalDEM topographic dataset, in contrast to the MERIT DEM dataset employed in this analysis (see Section 2). The results of this comparison are discussed in detail in Supplementary Materials Section S.1.2, Comparison of Inundation and Socioeconomic Impact Analyses with Different DEM Datasets.

3.4. Limitations

Due to the global scale of the studies which generated the present dataset, it should be regarded as a first-pass assessment of the global implications of ESL and coastal flooding over the next century. There are a number of factors which limit the global and regional outputs. A number of these limitations are summarized below, with a more extensive discussion by Kirezci et al. [5,7].

The ESL values were computed by fitting time-series data to EVA distributions (see Section 3), which results in stochastic uncertainty. A bootstrapping approach was used by Kirezci et al. [5] to estimate the resulting confidence limits.

Future estimates of sea level rise are associated with projection uncertainty. To address the sensitivities to possible errors, two global projections of RSLR (SROCC and AR5) were used for the present analysis. The implications of the two datasets are discussed in detail by Kirezci et al. [7]. Although both sources demonstrate relatively similar global mean projections [1], there are some regional differences, with SROCC end-century projections tending to be slightly higher than in AR5. To determine potential uncertainties associated with the full analysis used to generate the present dataset, the analysis was repeated with the 5th, 50th, and 95th percentile limits given by SROCC and AR5. Note that the data related to the 5th and 95th percentile limits are not provided within this dataset; however, the resulting confidence bands are discussed by Kirezci et al. [7].

As noted above, topography data are possibly the greatest source of uncertainty in coastal flooding studies. Both MERIT and CoastDEM terrain models were used in this study and the potential uncertainties are considered in Figure S2. The CoastDEM results are not included in the present database.

To determine the flood extent, we applied a bathtub approach, where the ESL exceeds the coastal defence structure and flood depth. In this approach, the storm duration and potential sea level attenuation are neglected. In reality, storm duration, the height of the coastal defence structure, and the geographical conditions of the shore (e.g., whether it is mangrove, etc.) will impact the flood depth behind any coastal defence. Although the bathtub approach is usually assumed to overpredict the inundation extent [30] by potentially underestimating impacts like overland flood attenuation [40], this approach is the only practical approach for global-scale analysis.

Land subsidence due to anthropogenic groundwater or gas extraction is not included in the present ESL dataset, which may result in an underestimation of the flood extent and potential impacts [14,41,42].

Despite these limitations [5,7], the present dataset compares well against tide gauge data and is consistent with a broad range of previous studies. As such, the dataset represents a plausible first-pass projection of the impacts of coastal flooding in the coming century.

3.5. Technical Background to the Data Visualization in the Digital Twin Platform

In addition to the data records described below, a data visualization system has also been developed for potential users. Figure 2 illustrates the communication between the coastal flood data housed in the Digital Twin servers and the client. The process comprises three elements: the database (or raw data file), web map services and web map client. On the backend-server side, the coastal flood datasets are hosted either on GeoDatabases or as Shapefiles. Both formats are directly linked to the GeoServer as a data store and published through OGC (Open Geospatial Consortium) standards such as the Web Map Service (WMS) and Web Map Tile Service (WMTS). The Digital Twin client is web browser-based and serves a map client integrated with a 3D globe visualization engine Cesium (www.cesium.com), which provides capabilities for spatial data visualization and spatial data query in a true 3D environment. To host and visualize global coverage data, like coastal flood data, the Digital Twin client has been optimized using the following methods. Firstly, all the web map tiles are pre-rendered and cached on the server side and delivered through WMTS to reduce the rendering pressure on the client side. Secondly, map tiles are loaded on the client side based on zoom level and bounding box to boost the loading performance and reduce the network traffic. Thirdly, map feature information, including geometry and attributes, has been designed to be displayed on demand for spatial data queries through GetFeatureInfo operations of WMTS to enable interactive data query and visualization.

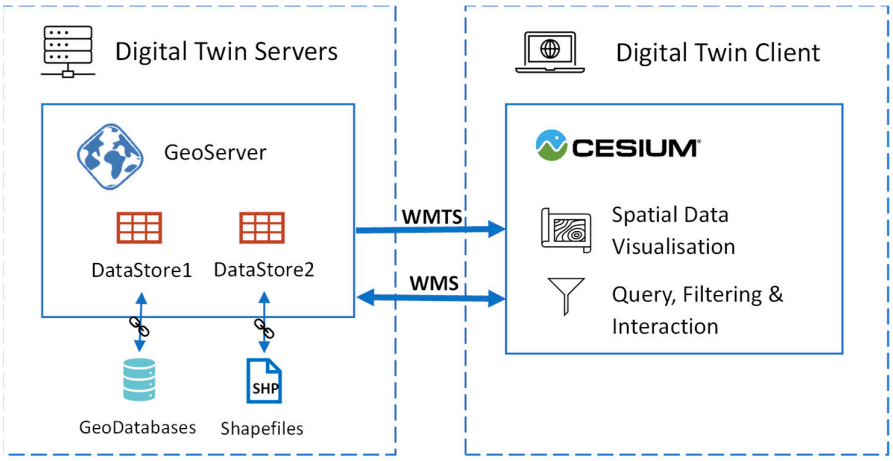

Figure 2. Data Hosting and visualising on the Digital Twin Platform visualization system.

4. User Notes

This section describes how to use the online interactive flood visualization tool, CoastalFloodPlatform.

The tool can be accessed at: https://idigitaltwin.org/?view=coastalFloodViewer (accessed on 24 January 2025)

Users are advised to exercise caution in the use of the present datasets. This global coastal flooding data and the visualization tool and maps are provided for a macroscopic portrayal of coastal flood risk and are unsuitable for localized assessments due to their inherent low resolution. Please note that the coarse resolution of the data and the approximations used for a global representation of coastal protection levels are unsuitable for finer-scale investigations. It is crucial to acknowledge that this dataset and its corresponding maps are not designed for localized applications, and users are encouraged to exercise caution, particularly when interpreting the data at regional or smaller scales. The developers make no expressed or implied warranties with respect to the accuracy, completeness, character, function or capabilities of the online tool or the data. Appropriate use and conclusions drawn from the data and images are the responsibility of the user.

The Coastal Flooding Platform comprises 3 main layers:

- Extreme sea levels at point locations (under the "Extreme Sea Levels" tab);
- Flood areas for different adaptation scenarios (under "Flood Areas—Baseline", "Flood Areas with Adaptation" and "Flood Areas without Adaptation" tabs);
- Aggregated data of Expected Annual Damage and Expected Annual People Affected at country levels for different adaptation scenarios (under the "Adaptation Scenarios" tab).

General usage notes:

1. The users must read and understand the disclaimer before viewing the platform.
2. The user can choose any of the data sets in the Coastal Flood Menu on the left handside, and the data will be rendered for the whole domain.
3. Note that, the EAPA and EAD values for all the adaptation scenarios (for 2050 and 2100) are provided as relative to the present case (baseline).
4. The map base can be shown as a 3D view or a 2D view using the  icon in the toolbox.
5. The flooded areas can be compared against each other, e.g., Baseline RP100 and RP10000. This can be done using the split view  in the toolbox menu. The two map areas then can be compared against each other by sliding the split view cursor.

6. The legend for all datasets can be added by icon.
7. The related publications and the datasets that are utilized in this platform can be accessed using icon.

Supplementary Materials: The following supporting information can be downloaded at https://www.mdpi.com/article/10.3390/data10020015/s1.

Author Contributions: Conceptualization, I.Y. and E.K.; methodology, I.Y. and E.K.; visualization, Y.C., Y.Z. and A.R.; writing—original draft preparation, E.K., I.Y., R.R., Y.C., Y.Z. and A.R.; writing—review and editing, E.K., I.Y., R.R., Y.C., Y.Z. and A.R. All authors have read and agreed to the published version of the manuscript.

Funding: I.Y. gratefully acknowledges the support of the Australian Research Council through grants DP130100215, DP160100738 and DP210100840. R.R. is supported by the AXA Research Fund and the Deltares Strategic Research Programme "Risk Management". The GOW2 data used to determine the breaking wave setup was generously supplied by Melisa Menendez. The storm surge data used to determine the global extreme flooding levels was provided by Sanne Muis.

Data Availability Statement: The data presented in this paper is available through the following link: https://doi.org/10.26188/25874179.v1. The publicly available datasets are described in the "Section 3".

Acknowledgments: The GOW2 data used to determine breaking wave setup were generously supplied by Melisa Menendez. The storm surge data used to determine the global extreme flooding levels were provided by Sanne Muis.

Conflicts of Interest: The authors declare no conflicts of interest.

References

1. Oppenheimer, M.; Glavovic, B.; Hinkel, J.; van der Wal, R.; Magnan, A.; Abd-Elgawad, A.; Cai, M.C.-J.R. Sea Level Rise and Implications for Low-Lying Islands, Coasts and Communities. In *The Ocean and Cryosphere in a Changing Climate: Special Report of the Intergovernmental Panel on Climate Change*; Pörtner, H.-O., Roberts, D.C., Masson-Delmotte, V., Zhai, P., Tignor, M., Poloczanska, E., Mintenbeck, A., Alegría, A., Nicolai, M., Okem, A., et al., Eds.; Cambridge University Press: Cambridge, UK; New York, NY, USA, 2019; pp. 321–445. [CrossRef]
2. Rasmussen, D.J.; Bittermann, K.; Buchanan, M.; Kulp, S.; Strauss, B.; Kopp, R.; Oppenheimer, M. Extreme sea level implications of 1.5 C, 2.0 C, and 2.5 C temperature stabilization targets in the 21st and 22nd centuries. *Environ. Res. Lett.* **2018**, *13*, 034040. [CrossRef]
3. Tebaldi, C.; Ranasinghe, R.; Vousdoukas, M.; Rasmussen, D.J.; Vega-Westhoff, B.; Kirezci, E.; Kopp, R.E.; Sriver, R.; Mentaschi, L. Extreme sea levels at different global warming levels. *Nat. Clim. Change* **2021**, *11*, 746–751. [CrossRef]
4. Vitousek, S.; Barnard, P.L.; Fletcher, C.H.; Frazer, N.; Erikson, L.; Storlazzi, C.D. Doubling of coastal flooding frequency within decades due to sea-level rise. *Sci. Rep.* **2017**, *7*, 1399. [CrossRef] [PubMed]
5. Kirezci, E.; Young, I.R.; Ranasinghe, R.; Muis, S.; Nicholls, R.J.; Lincke, D.; Hinkel, J. Projections of global-scale extreme sea levels and resulting episodic coastal flooding over the 21st Century. *Sci. Rep.* **2020**, *10*, 11629. [CrossRef]
6. Almar, R.; Ranasinghe, R.; Bergsma, E.W.J.; Diaz, H.; Melet, A.; Papa, F.; Vousdoukas, M.; Athanasiou, P.; Dada, O.; Almeida, L.P.; et al. A global analysis of extreme coastal water levels with implications for potential coastal overtopping. *Nat. Commun.* **2021**, *12*, 3775. [CrossRef]
7. Kirezci, E.; Young, I.R.; Ranasinghe, R.; Lincke, D.; Hinkel, J. Global-scale analysis of socioeconomic impacts of coastal flooding over the 21st century. *Front. Mar. Sci.* **2023**, *9*, 1024111. [CrossRef]
8. Vousdoukas, M.I.; Mentaschi, L.; Voukouvalas, E.; Verlaan, M.; Feyen, L. Extreme sea levels on the rise along Europe's coasts. *Earth's Future* **2017**, *5*, 304–323. [CrossRef]
9. Wolff, C.; Vafeidis, A.T.; Muis, S.; Lincke, D.; Satta, A.; Lionello, P.; Jimenez, J.A.; Conte, D.; Hinkel, J. A Mediterranean coastal database for assessing the impacts of sea-level rise and associated hazards. *Sci. Data* **2018**, *5*, 180044. [CrossRef]
10. Taherkhani, M.; Vitousek, S.; Barnard, P.L.; Frazer, M.; Fletcher, C. Sea-level rise exponentially increases coastal flood frequency. *Sci. Rep.* **2020**, *10*, 6466. [CrossRef]

11. Muis, S.; Verlaan, M.; Winsemius, H.; Aerts, J.C.J.H.; Ward, P.J. A global reanalysis of storm surges and extreme sea levels. *Nat. Commun.* **2016**, *7*, 11969. [CrossRef]
12. Vousdoukas, M.I.; Mentaschi, L.; Voukouvalas, E.; Verlaan, M.; Jevrejeva, S.; Jackson, L.P.; Feyen, L. Global probabilistic projections of extreme sea levels show intensification of coastal flood hazard. *Nat. Commun.* **2018**, *9*, 2360. [CrossRef] [PubMed]
13. Muis, S.; Verlaan, M.; Nicholls, R.J.; Brown, S.; Hinkel, J.; Lincke, D.; Vafeidis, A.T.; Scussolini, P.; Winsemius, H.C.; Ward, P.J. A comparison of two global datasets of extreme sea levels and resulting flood exposure. *Earth's Future* **2017**, *5*, 379–392. [CrossRef]
14. Tiggeloven, T.; de Moel, H.; Winsemius, H.C.; Eilander, D.; Erkens, G.; Gebremedhin, E.; Loaiza, A.D.; Kuzma, S.; Luo, T.; Iceland, C.; et al. Global-scale benefit–cost analysis of coastal flood adaptation to different flood risk drivers using structural measures. *Nat. Hazards Earth Syst. Sci.* **2020**, *20*, 1025–1044. [CrossRef]
15. Hinkel, J.; Lincke, D.; Vafeidis, A.; Perrettec, M.; Nicholls, R.; Tole, R.; Marzeiong, B. Coastal flood damage and adaptation costs under 21st century sea-level rise. *Proc. Nat. Acad. Sci. USA* **2014**, *111*, 3292–3297. [CrossRef]
16. Church, J.A.; Clark, P.; Cazenave, A.; Gregory, J.; Jevrejeva, S.; Levermann, A.; Merrifield, M.; Milne, G.; Nerem, R.S.; Nunn, P.; et al. *Climate Change 2013: The Physical Science Basis. Contribution of Working Group I to the Fifth Assessment Report of the Intergovernmental Panel on Climate Change*; Cambridge University Press: New York, NY, USA, 2013; pp. 1137–1216.
17. Carrere, L.; Lyard, F.; Cancet, M.; Guillot, A.; Picot, N. FES 2014, a new tidal model-Validation results and perspectives for improvements. In Proceedings of the ESA Living Planet Conference, Prague, Czech Republic, 9–13 May 2016.
18. Dee, D.P.; Uppala, S.M.; Simmons, A.J.; Berrisford, P.; Poli, P.; Kobayashi, S.; Andrae, U.; Balmaseda, M.A.; Balsamo, G.; Bauer, P.; et al. The ERA-Interim reanalysis: Configuration and performance of the data assimilation system. *Q. J. R. Meteorol. Soc.* **2011**, *137*, 553–597. [CrossRef]
19. Perez, J.; Menendez, M.; Losada, I.J. GOW2: A global wave hindcast for coastal applications. *Coast. Eng.* **2017**, *124*, 1–11. [CrossRef]
20. US Army Corps of Engineers. *Shore Protection Manual*, 4th ed.; U.S. Government: Washington, DC, USA, 1984.
21. Stockdon, H.F.; Holman, R.A.; Howd, P.A.; Sallenger, A.H., Jr. Empirical Parameterization of setup, swash, and runup. *Coast. Eng.* **2006**, *53*, 573–588. [CrossRef]
22. Woodworth, P.L.; Hunter, J.R.; Marcos, M.; Caldwell, P.; Menéndez, M.; Haigh, I. Towards a global higher-frequency sea level dataset. *Geosci. Data J.* **2016**, *3*, 50–59. [CrossRef]
23. Rio, M.; Mulet, S.; Picot, N. Beyond GOCE for the ocean circulation estimate: Synergetic use of altimetry, gravimetry, and in situ data provides new insight into geostrophic and Ekman currents. *Geophys. Res. Lett.* **2014**, *41*, 8918–8925. [CrossRef]
24. Yamazaki, D.; Ikeshima, D.; Tawatari, R.; Yamaguchi, T.; O'Loughlin, F.; Neal, J.C.; Sampson, C.C.; Kanae, S.; Bates, P.B. A high-accuracy map of global terrain elevations. *Geophys. Res. Lett.* **2017**, *44*, 5844–5853. [CrossRef]
25. Jarvis, A.; Reuter, H.I.; Nelson, A.; Guevara, E. Hole-Filling SRTM for the Globe, Version 4. 2008. Available online: http://srtm.csi.cgiar.org (accessed on 25 October 2024).
26. Farr, T.G.; Rosen, P.; Caro, E.; Crippen, R.; Duren, R.; Hensley, S.; Kobrick, M.; Paller, M.; Rodriguez, E.; Roth, L.; et al. The shuttle radar topography mission. *Rev. Geophys.* **2007**, *45*, 1–33. [CrossRef]
27. Kulp, S.A.; Strauss, B.H. CoastalDEM v2.1: A High-Accuracy and -Resolution Global Coastal Elevation Model Trained on ICESat-2 Satellite Lidar. 2021. Available online: http://www.climatecentral.org/coastaldem-v2.1 (accessed on 25 October 2024).
28. Wessel, P.; Smith, W.H.F. A Global Self-consistent, Hierarchical, High-resolution Shoreline Database. *J. Geophys. Res.* **1996**, *101*, 8741–8743. [CrossRef]
29. Vafeidis, A.T.; Nicholls, R.J.; McFadden, L.; Tol, R.S.J.; Hinkel, J.; Spencer, T.; Grashoff, P.S.; Boot, G.; Klein, R.J.T. A new global coastal database for impact and vulnerability analysis to sea-level rise. *J. Coast. Res.* **2008**, *244*, 917–924. [CrossRef]
30. Vousdoukas, M.I.; Voukouvalas, E.; Mentaschi, L.; Dottori, F.; Giardino, A.; Bouziotas, D.; Bianchi, A.; Salamon, P.; Feyen, L. Developments in large-scale coastal flood hazard mapping. *Nat. Hazards Earth Syst. Sci.* **2016**, *16*, 1841–1853. [CrossRef]
31. Gao, J. *Downscaling Global Spatial Populationn Projections from 1/8-Degree to 1-km Grid Cells*; NCAR Technical Note, NCAR/TN-537+5TR; National Center for Atmospheric Research: Boulder, CO, USA, 2017; 9p. [CrossRef]
32. Kummu, M.; Taka, M.; Guillaume, J.H.A. Gridded global datasets for Gross Domestic Product and Human Development Index over 1990–2015. *Sci. Data* **2018**, *5*, 180004. [CrossRef]
33. Riahi, K.; Van Vuuren, D.P.; Kriegler, E.; Edmonds, J.; O'Neill, B.C.; Fujimori, S.; Bauer, N.; Calvin, K.; Dellink, R.; Fricko, O.; et al. The Shared Socioeconomic Pathways and their energy, land use, and greenhouse gas emissions implications: An overview. *Glob. Environ. Change* **2017**, *42*, 153–168. [CrossRef]
34. Hinkel, J.; Klein, R. Integrating knowledge to assess coastal vulnerability to sea-level rise: The development of the DIVA tool. *Glob. Environ. Change* **2009**, *19*, 384–395. [CrossRef]
35. Sadoff, C.W.; Hall, J.; Grey, D.; Aerts, J.; Ait-Kadi, M.; Brown, C.; Cox, A.; Dadson, S.; Garrick, D.; Kelman, J.; et al. *Securing Water, Sustaining Growth: Report of the GWP/OECD Task Force on Water Security and Sustainable Growth*; University of Oxford: Oxford, UK, 2015.

36. Hallegatte, S.; Green, C.; Nicholls, R.J.; Corfee-Morlot, J. Future flood loses in major coastal cities. *Nat. Clim. Change* **2013**, *3*, 802–806. [CrossRef]
37. Meyer, V.; Scheuer, S.; Haase, D. A multicriteria approach for flood risk mapping exemplified at the Mulde river, Germany. *Nat. Hazards* **2008**, *48*, 17–39. [CrossRef]
38. Zhou, Q.; Mikkelsen, P.M.; Halsnæs, K.; Arnbjerg-Nielsen, K. Framework for economic pluvial flood risk assessment considering climate change effects and adaptation benefits. *J. Hydrol.* **2012**, *414–415*, 539–549. [CrossRef]
39. Muis, S.; Güneralp, B.; Jongman, B.; Aerts, J.C.; Ward, P.J. Flood risk and adaptation strategies under climate change and urban expansion: A probabilistic analysis using global data. *Sci. Total Environ.* **2015**, *538*, 445–457. [CrossRef] [PubMed]
40. Vafeidis, A.; Schuerch, M.; Wolff, C.; Spencer, T.; Merkens, J.; Hinkel, J.; Lincke, D.; Brown, S.; Nicholls, R. Water-level attenuation in global-scale assessments of exposure to coastal flooding: A sensitivity analysis. *Nat. Hazards Earth Syst. Sci.* **2019**, *19*, 973–984. [CrossRef]
41. Ericson, J.; Vorosmarty, C.; Dingman, S.; Ward, L.; Meybeck, M. Effective sea-level rise and deltas: Causes of change and human dimension implications. *Glob. Planet. Change* **2006**, *50*, 63–82. [CrossRef]
42. Syvitski, J.P.M.; Kettner, A.J.; Overeem, I.; Hutton, E.W.H.; Hannon, M.T.; Brakenridge, G.R.; Day, J.; Vörösmarty, C.; Saito, Y.; Giosan, L.; et al. Sinking deltas due to human activities. *Nat. Geosci.* **2009**, *2*, 681–686. [CrossRef]